

Sol-gel particle growth studied using fluorescence anisotropy: An alternative to scattering techniques

David J. S. Birch* and Chris D. Geddes

The Photophysics Group, Department of Physics and Applied Physics, Strathclyde University, Glasgow G4 0NG, Scotland

(Received 16 April 1999)

The aggregation of silica particles during hydrogel polymerization has been observed *in situ* with angstrom resolution using the combined fluorescence anisotropy decay of solvated and bound dye. Primary particles of mean hydrodynamic radius ≈ 1.5 nm are found to be present within 20 min of mixing sodium silicate solution and sulfuric acid. Clustering then occurs during siloxane polymerization to produce after ≈ 30 h secondary particles with a mean radius up to ≈ 4.5 nm at a growth rate that depends on silicate concentration and time to microgelation t_g . Subsequent condensation to ≈ 4 nm radius occurs within 1 week as particle syneresis dominates.

PACS number(s): 83.70.Hq, 82.70.Dd

There can be few more important materials than silica and water. The former constitutes the most abundant material in the earth's crust and the latter occupies most of the surface of the earth. The properties of the two are inextricably linked in the search for a better understanding of the molecular dynamics responsible for sol to gel phase transitions. Few techniques permit the study of both, but in this paper we report the results of an approach that gives independent, simultaneous, and *in situ* characterization of the aqueous phase and silica particle size during sol-gel polymerization.

The sol-gel process is a room temperature inorganic polymerization involving a series of hydrolysis and condensation steps to produce a rigid network. It owes its origins to the pioneering work of Ebelman, Mendeleev, and Graham in the 19th century [1]. The sol to gel transition is characterized by a gel point, after a time t_g , at which a fine silica network spans the containing vessel. Of all the possible syntheses, the mixing of concentrated sulfuric acid and sodium silicate (i.e., water glass) to produce silica gel, through the formation of siloxane ($-\text{Si}-\text{O}-\text{Si}-$) bonds, has the largest industrial significance owing to the large scale production of silica gel for everyday applications such as an abrasive, filling, and refining agent. Hence, although possessing an ill-defined starting point by virtue of having a range of initial species [1], it is perhaps somewhat surprising that silica hydrogel dynamics have received such little attention in the research literature. Over the past two decades the picture has emerged of acidic silica hydrogels (i.e., at $\text{pH} < 2$) being formed by the coalescence of nanometer scale polymer particles containing ≈ 4 or 5 silica tetrahedra [2] to form secondary particles rather than through the extension and cross-linking of polymer chains as is the case for organic polymers [1]. Brinker and Scherer [1] have documented the effect of pH and surface charge on t_g and particle growth. At $\text{pH} \approx 2$ the surface charge is neutral, becoming slightly positive at $\text{pH} < 2$ (acidic gels), resulting in long gel times and little particle growth other than through aggregation. The surface charge is negative at $\text{pH} > 2$, facilitating more rapid gelation

up to $\text{pH} 6$. At $\text{pH} > 7$ particles are highly anionic, mutually repulsive, form stable sols, and grow mainly by the dissolution of smaller particles and deposition of silica on larger particles due to solubility differences (Ostwald ripening).

Considerable effort has been applied to solutions of Smoluchowski's equation and computer simulations in order to model cluster growth [1]. Reaction- or diffusion-limited cluster-cluster aggregation (RLCA or DLCA) models [3], modified to take account of deformation due to rearrangement about the point of initial contact between clusters [4], have proved successful at describing the kinetic and structural processes prior to gelation. At $\text{pH} < 2$, the slightly positive repulsion between particles, which bind on collision according to the probability of an interparticle condensation reaction, is thought to lead to RLCA conditions, which predict growth [1] for nongelling systems described by a mean diameter $d \sim e^{ct}$. Conversely, DLCA predicts $d \sim t$. The lack of primary particle growth other than by aggregation at low pH makes acidic hydrogels ideal for studying cluster dynamics. However, the small size of primary particles makes the task difficult as subnanometer resolution is required to answer fundamental questions concerning silica hydrogenation and silica particle dimensions. For example, at what point are silica primary particles formed in the sol or are they already present in the silicate? What is the rate of change of particle size during polymerization? Is there a relationship between particle size, gelation time, and silicate concentration? We have sought to answer such questions by time-resolved fluorescence measurements on silica particles labeled with a fluorescent dye.

Changes in the decay of fluorescence anisotropy as polymerization proceeds are simply explained in terms of changes in the relative abundance of solvated dye and dye attached to silica particles. This dual behavior of the probe means that a single anisotropy decay measurement leads to determination of both the fluid microviscosity and the particle hydrodynamic radius. Although microviscosity in silica alkoxide alcogels has recently been studied using fluorescence anisotropy [5,6], no evidence for particles was reported. Also, fluorescence studies of silica hydrogels at $\text{pH} < 2$ are more difficult than for alkoxide alcogels because of

*Author to whom correspondence should be addressed.

hydrogel intrinsic fluorescence and the highly acidic nature, which can lead to chemical degradation of aromatic probes. We have overcome these problems using the xanthene type probe [7] JA120, which has fluorescence characteristics unperturbed by this harsh environment. The near infrared fluorescence of this dye (spectral peak at 690 nm) brings additional benefits, specifically, reduced Rayleigh scattering of excitation and fluorescence (λ^{-4} dependence), negligible sol-gel intrinsic fluorescence, and compatibility with diode laser excitation, such that fluorescence decays can be accurately measured in ≈ 2 min time windows, during which time any change in the sol-gel is minimized.

Different weight for weight concentrations of sulfuric acid and silicate (Crystal 79) were mixed together using stainless steel blades rotating at 1200 rpm and delivered at controlled flow rates using peristaltic pumps to produce specific sol-gels of differing t_g . For the results presented here the particle surface charge was kept effectively constant by keeping the excess acid normality in the final sol in the range between 0.25N and 0.31N (pH 0.9–0.81). The t_g for the sol compositions studied varied between ≈ 60 and 3000 min. Orthogonal polarized fluorescence decay curves were each recorded in ≈ 1 min, at different time delays following initial mixing of the sol using the time-correlated single-photon counting technique [8]. Excitation was provided by a Hamamatsu PLP-02 650 nm diode laser generating vertically polarized optical pulses of duration ≈ 50 ps at 1 MHz repetition rate. The detector was an EG&G CD2027 avalanche photodiode. The overall instrumental response function was ≈ 350 ps full width at half maximum. Fluorescence was selected using an IBH model 5000M $f/3$ monochromator, a Kodak 720 nm cutoff filter, and a Halbro Optics dichroic polarizer. Nonlinear least squares impulse deconvolution analysis of the anisotropy data [8] was performed using the IBH Ltd. fluorescence lifetime systems software library with a χ^2 goodness of fit criterion. For all the measurements ~ 4 cm³ of sol remained optically transparent in $1 \times 1 \times 4$ cm³ unsealed cuvettes as gelation and drying occurred, so that depolarization due to multiple scattering from particles and pores can be neglected.

Fluorescence depolarization can be represented by the reorientational correlation function [9] $r(t) = 0.4 \langle P_2[\mu_e(t) \cdot \mu_a(0)] \rangle$, where $\mu_e(t)$ and $\mu_a(0)$ are the emission and absorption dipoles at time t and time zero, respectively, and P_2 is the second order Legendre polynomial. A dye bound to a silica particle can be described well by the Brownian isotropic rotation of a sphere, such that the usual three diffusion tensors are reduced to one, D , giving the Perrin equation for the decay of fluorescence anisotropy [10],

$$r(t) = r_0 e^{-6Dt}, \quad (1)$$

where r_0 is the initial anisotropy with a maximum value of 0.4 and, in the simplest case, the rotational correlation time τ_r is described by the Stokes-Einstein equation,

$$\tau_r = (6D)^{-1} = \eta V / kT, \quad (2)$$

where η is the microviscosity, V the hydrodynamic volume, T the temperature and k the Boltzmann constant. By recording vertically and horizontally polarized fluorescence decay curves $F_V(t)$ and $F_H(t)$ orthogonal to vertically polarized

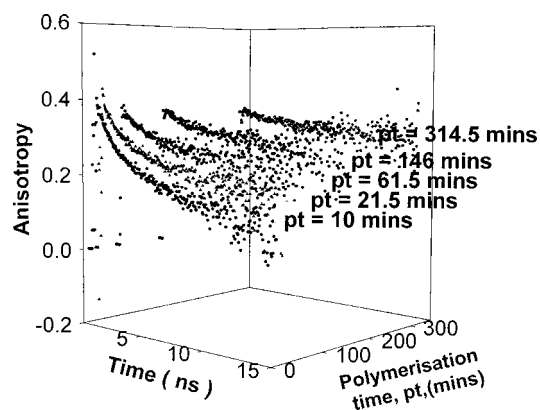


FIG. 1. Fluorescence anisotropy decay curves as function of polymerization time pt for a 15.3% SiO_2 and 0.27N sol-gel.

excitation, an anisotropy function $r(t) = [F_V(t) - F_H(t)] / [F_V(t) + 2F_H(t)]$ can be generated.

Our study of JA120 in a range of solvents showed it to be an isotropic rotor with a hydrodynamic radius of 7.5 Å, a figure we have used in subsequent viscosity calculations. JA120 is cationic and at the pH used in our measurements (< 1) the silica particles are slightly positive. This slight repulsion of the dye by the silica leads to a fraction f of the total fluorescence being due to the probe molecules bound to silica particles and hence $1-f$ due to probe molecules unbound in the sol. The anisotropy then takes the form

$$r(t) = (1-f)r_0 e^{-t/\tau_{r1}} + f r_0 e^{-t/\tau_{r2}}, \quad (3)$$

with τ_{r2} giving the particle radius, which can be derived from Eq. (2) after using τ_{r1} to determine the microviscosity of the aqueous phase of the sol.

Figure 1 shows typical anisotropy decay curves, illustrating the trends observed as polymerization proceeds for a 15.3% by weight SiO_2 concentration. Distinguishing between alternative kinetic models of two rotational correlation times and zero residual anisotropy [Eq. (3)] and one rotational time and nonzero residual anisotropy can be difficult to establish in a single measurement. Indeed, the two models are not necessarily mutually exclusive because, on longer time scales than we are able to observe the anisotropy with reasonable statistical precision (≈ 20 ns), a long rotational time could be equally well described by a residual anisotropy. This is because anisotropy information is available only during the short fluorescence decay of JA120 (lifetime in $\text{H}_2\text{O} \approx 1.83$ ns). However, for all the anisotropy decay curves, fitting to Eq. (3) consistently gave a better description (lower χ^2 value). Equation (3) was found to provide R_0 values closest to the theoretical maximum of 0.4 and reassuringly constant as f increases with time. Moreover, extension of Eq. (3) to include a fraction of fluorescence due to dye bound to the macronetwork in the gel was found to be inappropriate.

Precipitating silica at various times during the sol to gel transition by the addition of excess methanol confirmed the probe to be both free in solution and attached to silica, with more dye recovered in the methanol filtrate at earlier times. Figure 1 shows that the relative fluorescence intensity f due to the long rotational correlation time increases with polymerization time. These facts confirm that the fluorescence

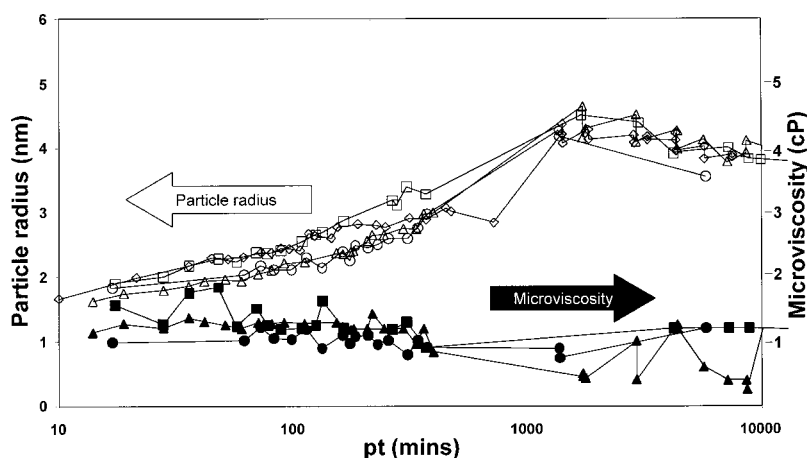


FIG. 2. Fluid microviscosity (solid symbols) and particle hydrodynamic mean radius (open symbols) as functions of polymerization time pt for 15.3% final SiO_2 concentration and 0.27N excess acid normality (viscosity omitted for clarity, radius \diamond), 12.7% SiO_2 and 0.25N (\blacksquare, \square), 9.14% SiO_2 and 0.31N ($\blacktriangle, \triangle$), 6.02% SiO_2 and 0.30N (\bullet, \circ) sol-gels. The corresponding t_g values are 60–74, 240–270, 990–1050, and 2760–3240 min, respectively.

anisotropy reflects the joint contributions of unbound probe rotating in the fluid and probe bound to silica particles. At long times nearly all the emission originates from dye bound to silica particles and Eq. (1) then gives quite a good fit to the anisotropy decay. We observed the total fluorescence count rate to increase during polymerization ($\approx 30\%$) and this probably reflects an increase in fluorescence quantum yield when the dye is bound to silica. For this reason the fraction f does not describe the fraction of the total number of probe molecules that are bound to silica.

We turn now to the rotational correlation times determined with Eq. (3). For a given sol, τ_{r1} was fairly constant within the range ≈ 0.5 –1 ns and this constancy within the error is illustrated in Fig. 2 for the corresponding microviscosity, derived from Eq. (2) to be in the range ~ 1 –2 cP. We associate τ_{r1} with the rotation of the probe in the fluid part of the sol and indeed in residual fluid in the gel. Hence the microviscosity is significantly less than the bulk viscosity at all times, and our interpretation finds no evidence for the coexistence of two viscosity domains as reported in alkoxide alcogels [6]. Despite the large errors there is some evidence in our data that the microviscosity is lowered during polymerization, consistent with the take up of silicate species from the fluid.

Figure 2 also shows how the mean particle hydrodynamic radius changes from the outset. From τ_{r1} we have calculated mean microviscosities in the temporal regions where they prevail for each sol and hence determined particle radius from τ_{r2} using Eq. (2). The maximum mean hydrodynamic radius of particles existing initially or formed within 20 min of mixing is ≈ 1.5 nm. We say “maximum” because we have made no allowance for the dimensions of the dye (≈ 0.7 nm). However, the dye might be expected to intercalate within the open form of such primary structures [1], thus adding little to the cluster diameter. Also, we have made no allowance for water molecules associated with the silica particles.

A striking feature of Fig. 2 is the near angstrom resolution of the mean particle radius, increasing from a minimum of ≈ 1.5 nm to a peak of ≈ 4.5 nm in ≈ 2000 min and then decreasing to ≈ 4 nm in ≈ 6000 min for all the sols. This suggests that the 4.5 nm clusters contain a maximum of ≈ 13 primary particles [11].

Unsealed cuvettes containing silica hydrogels typically show a 40% loss in weight due to water evaporation one

week after preparation. Although the increasing depolarization after 2000 min might be explained by an anomaly caused by depolarization due to dye-dye Förster nonradiative resonance energy transfer [8] as the dye aggregates, throughout the polymerization process we found no change in absorption spectrum of the dye, as would be indicative of dye clustering. Also, the rate of decay of anisotropy is constant after ≈ 6000 min despite the gel still drying and this is inconsistent with Förster energy transfer. Particle size reduction due to redissolution of silica seems unlikely (Ostwald ripening contributing little to the growth of primary particles at low pH [1]). Nor do we see either sieve deposition of the larger particles in the gel or reduction in the hydration sphere would be significant. Hence we propose that the size decrease we observe reflects the dominance of intraparticle syneresis over interparticle aggregation. Syneresis is a term more usually applied to gels, but at the molecular level it involves, in the simplest form, shrinkage via conversion of silanol groups, Si-OH , to siloxane —Si—O—Si— bridging bonds through polycondensation reactions [1]. Particle syneresis probably occurs from the outset, but is hidden at earlier times by aggregation. This implies that aggregation numbers for silica primary particles treated as solid spheres [11] may be slight underestimates. The aggregation rate would be expected to slow down as the number of particles decreases and the rate of particle syneresis slows down as all but any isolated hydroxyl groups are used up. Although not obvious on the $\log_{10} t$ axis of Fig. 2, the increase in particle mean radius is initially well described to a first order approximation by a function $r \approx r_0 + (r_{\text{max}} - r_0)(1 - e^{-kt})$, with r_0 values attributable to primary particles ranging from 1.4 to 1.7 nm (uncorrelated with $[\text{SiO}_2]$). The rate parameter k is $\approx 3.3 \times 10^{-5}$, 6.0×10^{-5} , 8.7×10^{-5} , and $1.7 \times 10^{-4} \text{ s}^{-1}$ for 6.02%, 9.14%, 12.7%, and 15.3% SiO_2 (weight for weight), respectively. Just before r_{max} the net k value is reduced by syneresis. The particle syneresis rate constant, assuming an exponential reduction in particle radius and that growth is absent after 30 hr, is $\approx 6.0 \times 10^{-6} \text{ s}^{-1}$. Particle syneresis is seen to be effectively over after ~ 100 h.

Only the growth rate k , but not r_0 or r_{max} , has any measurable dependence on $[\text{SiO}_2]$ or t_g , at t_g the sol still being much more abundant than the gel. The r_0 value of ≈ 1.5 nm that we detect is in close agreement with values reported from small angle scattering measurements made in many dif-

ferent laboratories over a range of sol-gel samples once the contribution of bound water to the hydrodynamic radius is considered. For example, light scattering measurements on a silicon alkoxide sol found a primary particle hydrodynamic diameter of 1.0 nm, increasing to 2.4 nm prior to gelation [12]. Small angle x-ray scattering studies of silica gel have revealed evidence for 1 nm particles [13] and similar studies on another alkoxide sol indicate that 2 nm diameter primary particles aggregate to form secondary particles of 6 nm diameter prior to gelation [14]. Small angle neutron scattering has produced comparable primary particle dimensions [15]. In one of the few studies on silica hydrogel formation, primary particles of ≈ 1 nm have been detected using x-ray scattering [16]. Based on this result and the initial hydrodynamic diameter of ≈ 3 nm, which we measure, this would correspond to a ≈ 1 -nm layer of bound water attached to the silica particles.

Similar particle growth curves to those we observe have been reported using electron microscopy on base catalyzed silicon alkoxide sols, but from an initial measurement of ≈ 100 nm [17], which means the growth function of the ≈ 1 nm primary particles was still not resolved. By choosing polymerization conditions that have a slow aggregation rate, we have been able to observe primary particle growth from the outset and secondary particle syneresis against a background

gel network. The condensation mechanism of growth and syneresis suggests that these observations are fundamental to sol-gel kinetics in general.

The method we describe is obviously useful in studying bound water and is in some ways much better placed than conventional techniques to record particle size *in situ* at high silicate concentrations and after gelation. Fluorescence depolarization is caused only by rotating particles. Conversely, to avoid multiple scattering, light scattering requires dilute silicates (dilution can cause depolymerization) and x-ray, neutron, and light scattering also occur from the gel network as well as particles. The technique we have described can be used for particle size measurement in any type of sol provided a suitable bound dye can be found, the maximum size of particle that can be resolved being determined only by the fluorescence lifetime of the dye.

We wish to acknowledge the EPSRC for research grants and financial support for C.D.G., the gift of the JA120 kindly made available to us by Dr. Jutta Arden-Jacob, University of Seigen, Germany, and technical support by J. Revie in helping to construct the sol-gel preparation rig. The comments and support of D. Ward of Unilever, and D. Aldcroft, I. McKeown, N. Rhodes, and A. Minihan of Crosfield Ltd. are gratefully acknowledged.

-
- [1] C. J. Brinker and G. Scherer, *Sol-Gel Science, The Physics and Chemistry of Sol-Gel Processing* (Academic, San Diego, 1989).
- [2] J. K. West, B. F. Zhu, Y. C. Cheng, and L. Hench, *J. Non-Cryst. Solids* **121**, 51 (1990).
- [3] P. Meakin, *Phys. Rev. Lett.* **51**, 1119 (1983).
- [4] R. Jullien, and A. Hasmy, *Phys. Rev. Lett.* **74**, 4003 (1995).
- [5] B. Dunn and J. I. Zink, *J. Mater. Chem.* **1**, 903 (1991).
- [6] F. V. Bright, U. Narang, R. Wang, and P. N. Prasad, *J. Phys. Chem.* **98**, 17 (1994).
- [7] K. H. Drexhage, N. J. Marx, and J. Arden-Jacob, *J. Fluoresc.* **7**, 91S (1997).
- [8] D. J. S. Birch and R. E. Imhof, in *Topics in Fluorescence Spectroscopy*, edited by J. R. Lakowicz (Plenum, New York, 1991), Vol. 1, p. 1.
- [9] A. Szabo, *J. Chem. Phys.* **81**, 150 (1984).
- [10] A. Kawaski, *Crit. Rev. Anal. Chem.* **23**, 459 (1993).
- [11] D. E. G. Williams, *J. Non-Cryst. Solids* **86**, 1 (1986).
- [12] A. H. Boonstra, T. P. M. Meeuwse, J. M. E. Baken, and G. V. A. Aben, *J. Non-Cryst. Solids* **109**, 153 (1989).
- [13] B. Himmel, Th. Gerber, and H. Bürger, *J. Non-Cryst. Solids* **91**, 122 (1987).
- [14] G. Orcel, L. L. Hench, I. Artaki, J. Jonas, and T. W. Zerda, *J. Non-Cryst. Solids* **105**, 223 (1988).
- [15] R. Winter, D.-W. Hua, P. Thiyagarajan, and J. Jonas, *J. Non-Cryst. Solids* **108**, 137 (1989).
- [16] Th. Gerber, B. Himmel, and C. Hübert, *J. Non-Cryst. Solids* **175**, 160 (1994).
- [17] G. H. Bogush and C. F. Zukoski, *J. Colloid Interface Sci.* **142**, 1 (1991).